Nanoscale

Accepted Manuscript

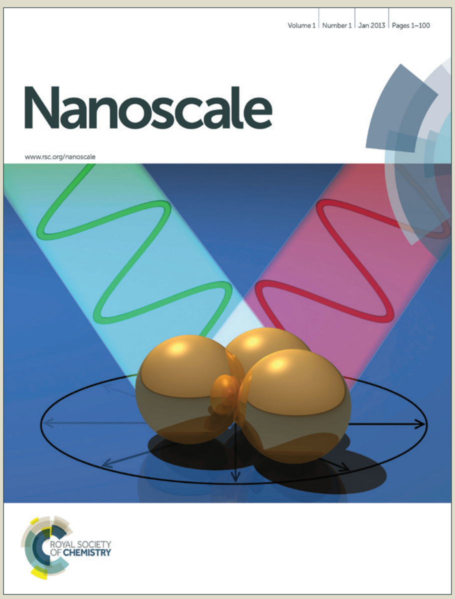

This is an *Accepted Manuscript*, which has been through the Royal Society of Chemistry peer review process and has been accepted for publication.

Accepted Manuscripts are published online shortly after acceptance, before technical editing, formatting and proof reading. Using this free service, authors can make their results available to the community, in citable form, before we publish the edited article. We will replace this *Accepted Manuscript* with the edited and formatted *Advance Article* as soon as it is available.

You can find more information about *Accepted Manuscripts* in the Information for Authors.

Please note that technical editing may introduce minor changes to the text and/or graphics, which may alter content. The journal's standard Terms & Conditions and the Ethical guidelines still apply. In no event shall the Royal Society of Chemistry be held responsible for any errors or omissions in this *Accepted Manuscript* or any consequences arising from the use of any information it contains.

ROYAL SOCIETY OF CHEMISTRY

www.rsc.org/nanoscale

Nanoscale RSCPublishing

ARTICLE

Tunable and rapid self-assembly of block copolymers using mixed solvent vapors†

Cite this: DOI: 10.1039/x0xx00000x

Received 00th January 2012,
Accepted 00th January 2012

DOI: 10.1039/x0xx00000x

www.rsc.org/

Woon Ik Park,[a] Sheng Tong,[b] Yuzi Liu,[b] Il Woong Jung,[b] Andreas Roelofs,[b] and Seungbum Hong*[a]

Pattern generation of well-controlled block copolymers (BCPs) with high Flory-Huggins interaction parameter (χ) is important for applications in sub-20 nm nanolithography. We used mixed solvents of dimethylformamide (DMF) and toluene to control the morphology as well as the time to achieve the targeted morphology *via* self-assembly of BCPs. By precisely controlling the volume ratio of DMF and toluene, well-ordered line, honeycomb, circular hole, and lamellar nanostructures were obtained from a cylinder-forming poly(styrene-*b*-2vinylpyridine) (PS-*b*-P2VP) BCP with high-χ. Furthermore, a well-aligned 12nm line pattern was successfully achieved in the guiding template within one minute by using the mixed solvents. This practical method may also be applicable to self-assembly of other BCPs, providing more opportunities for the next-generation sub-10 nm lithography applications.

Nanoscale Accepted Manuscript

Introduction

For the last several decades, the directed self-assembly (DSA) of block copolymers (BCPs) has attracted much attention due to its excellent ability to overcome the challenges of conventional semiconductor manufacturing process.[1-10] BCP which consists of two or more immiscible polymeric blocks can spontaneously self-assemble into well-organized nanostructures in the shape of dots, lines, circular holes, and lamellae with sub-20 nm feature sizes through a minimization of free energy.[3, 5, 8, 9, 11-20] Due to the great pattern resolution, scalability, and cost-effectiveness, the BCP self-assembly is one of the most promising candidates for next-generation lithography.[21-24] However, there are still several challenges to be solved such as defects, controllability, and self-assembly kinetics for wider applications of DSA.[21, 25, 26] Hence, many BCP research groups pay extensive efforts to resolve these existing issues.[13, 22, 23, 25, 27, 28-31]

To produce well-aligned patterns, chain mobility of BCP is increased mostly by thermal annealing or solvent vapor annealing. Especially for BCPs with a high Flory-Huggins interaction parameter (χ), which can create patterns with a small pitch, solvent vapor annealing is required to offer better chain flexibility and diffusivity.[13, 32-34] The geometry of the self-assembled BCP is variable generally depending on length of the chain and volume fraction of BCP, and therefore the self-assembled BCP has a limited set of morphologies for each kind of BCP.[35-37] However, as we previously reported,[13, 34, 38] geometrical tunability of BCPs with high-χ can be easily achieved through solvent vapor annealing with mixed solvent vapors composed of selectively swelling solvent molecules for each block of the BCP. In spite of these important advantages, solvent vapor annealing has a limitation in the self-assembly kinetics for high-χ BCPs. Recently, several BCP research groups reported how to improve processing time up to a few minutes for BCPs with high-χ to obtain well-ordered nanostructures using thermally-assisted solvent (solvothermal) annealing or microwave-driven fast self-assembly processes.[22, 23, 27, 28] Gotrik *et al.* demonstrated fast formation of well-ordered BCP structures using solvent annealing on the voltage-driven hot stage,[28] while Park *et al.* developed the self-assembly kinetics of solvent-induced BCP formation by temperature on the hot plate.[22] Zhang *et al.* reported rapid defect annihilation of BCPs by application of microwave annealing.[23] These results comprehensively showed that thermallyactivated solvent vapors can enhance the BCP self-assembly kinetics, showing smaller activation energy for chain diffusion.[39, 40] These studies suggest that we need more useful and convenient approach to realize rapid self-assembly of BCPs with high-χ as well as morphological controllability.

Here, we introduce a simple and practical pathway involving tunable and rapid self-assembly of BCPs with high-χ parameter. We systematically investigated how two mixed solvents can affect the morphology of BCPs in the solvent vapor annealing system, showing wide tunability (cylinder-to-lamella morphology transition) from a cylinder-forming poly(styrene-*b*-2vinylpyridine) (PS-*b*-P2VP) BCP with high-χ (~0.18)[41] and ultrafast self-assembly kinetics of the BCPs. Uniformly controlled honeycomb nanostructures arranged in six-fold symmetry were effectively obtained by optimizing the volume ratio of the mixed solvents. We also demonstrated how self-assembled pattern formation with a good order can be accomplished within one minute in the guiding templates using annealing of mixed solvent vapors.

Results and discussions

Fig. 1 presents morphology transitions of the cylinder-forming PS-*b*-P2VP BCP using mixed solvents of dimethylformamide (DMF) and toluene. To control the BCP morphology, we selected two organic solvents of DMF and toluene, which are preferential for P2VP and PS blocks, respectively. As shown in Fig. 1a, volumetric fraction of the BCP is variable depending on the volume ratio between DMF and toluene (V_{DMF}/V_{TOL}). When V_{DMF}/V_{TOL} ratio increases, effective volume fraction of P2VP block (f_{P2VP}^{eff}) is increased due to the selective swelling of P2VP by DMF during solvent annealing, leading to the morphological change from cylinder to lamella as shown in Figs. 1a-b. Fig. 1c shows the various self-assembled gold nanostructures of PS-*b*-P2VP (SV42) BCP with a molecular weight (MW) of 42 kg/mol and P2VP volume fraction of f_{P2VP}= 25%. For SV42 BCP, while well-ordered line pattern was formed when it was exposed to the pure toluene vapor (V_{DMF}/V_{TOL} = 0), hexagonally perforated lamellar (HPL) pattern was obtained when annealed at V_{DMF}/V_{TOL} = 0.71. The morphology underwent a considerable change as the fraction of DMF increased further ($V_{DMF}/V_{TOL} \geq$ 1), leading to the morphology transition to lamella (Fig. 1c, right).

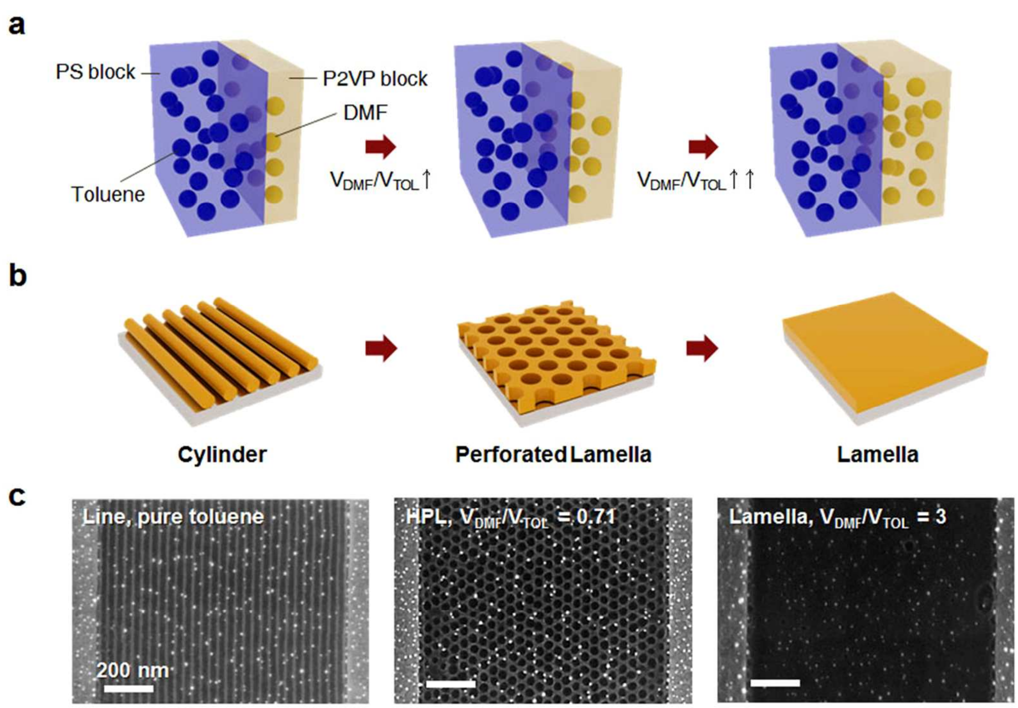

Fig. 1 Schematic of the self-assembled cylinder-forming PS-*b*-P2VP BCP using mixed solvents of DMF and toluene. (a) Effective volume fraction (f_{P2VP}^{eff}) increases in proportion to the V_{DMF}/V_{TOL}. (b) Morphological change from cylinder to lamella depending on the increase of f_{P2VP}. (c) SEM images for Au line (left), HPL (middle), and lamella (right) nanostructures.

Nanoscale Accepted Manuscript

 This journal is © The Royal Society of Chemistry 2014

Nanoscale RSCPublishing

ARTICLE

Fig. S1 shows the morphology evolution of the P2VP microdomain from HPL to lamella structure, as the fraction of DMF or f_{P2VP}^{eff} increases. Lamellar morphology began to appear at V_{DMF}/V_{TOL} = 1.0. When the BCP film was annealed at high volume ratio ($V_{DMF}/V_{TOL} \geq 2$), lamellar structure was obtained over the large area (Fig. S1d). These results suggest that self-assembly using mixed solvents can be a suitable and useful method to control the BCP morphology for BCPs with high-χ, showing wide morphological tunability.

In order to control the shape of circular hole in the HPL morphology, we precisely controlled the V_{DMF}/V_{TOL} ratio. Fig. 2a presents the evolution of the P2VP with holes uniformly arranged in a six-fold symmetry depending on the V_{DMF}/V_{TOL} ratio. While toluene vapor preferentially swells the PS block, DMF vapor selectively swells the P2VP block. When SV42 BCP was annealed at V_{DMF}/V_{TOL} = 0.71, conventional HPL structure with circular holes was formed with an average diameter of 38nm, center-to-center distance of 46 nm, and minimum line-width of 9.6 nm, respectively (Fig. 2a, top). However, after the BCP was annealed at the higher toluene or lower DMF portion (V_{DMF}/V_{TOL} = 0.62), the circular hole changed to the hexagon hole, which forms the basis of a honeycomb network as shown in the middle of Fig. 2a. It should be noted that the stretching energy of P2VP domain prefers a more uniform line thickness, leading to the formation of hexagonal hole structure.[42] For the discrete formation of the P2VP network, it is likely due to the excessive swelling of PS block, resulting from the high vapor pressure during solvent annealing process. The honeycomb network has narrower line-width (4.8 nm), while the center-to-center distance was the same as 38 nm regardless of the V_{DMF}/V_{TOL} ratio in the ratio of 0.5 – 0.71. At V_{DMF}/V_{TOL} = 0.5, the line width of the honeycomb was shrunk to 2 – 3 nm, showing well-organized honeycomb nanostructures with uniform hexagonal holes (Fig. 2a, bottom). For the discrete formation of the P2VP network, it is likely due to the high vapor pressure during solvent annealing process. Fig. 2b shows that honeycombs structures can be formed over the large area. Here, it should be noted that high-χ BCP can be successfully tuned by precisely controlling selective-swelling of each block. Moreover, the self-assembled nanostructures from PS-*b*-P2VP can form various metal or metal-oxide nanostructures (Pt, gold, Co, Fe, and so on) by selectively incorporating metal ions into P2VP block,[43] resulting in CoO_x and FeO_x nanostructures as shown in Fig. S2. Thus, this approach maybe extendable to device applications such as nonvolatile memories, solar cells, and batteries.

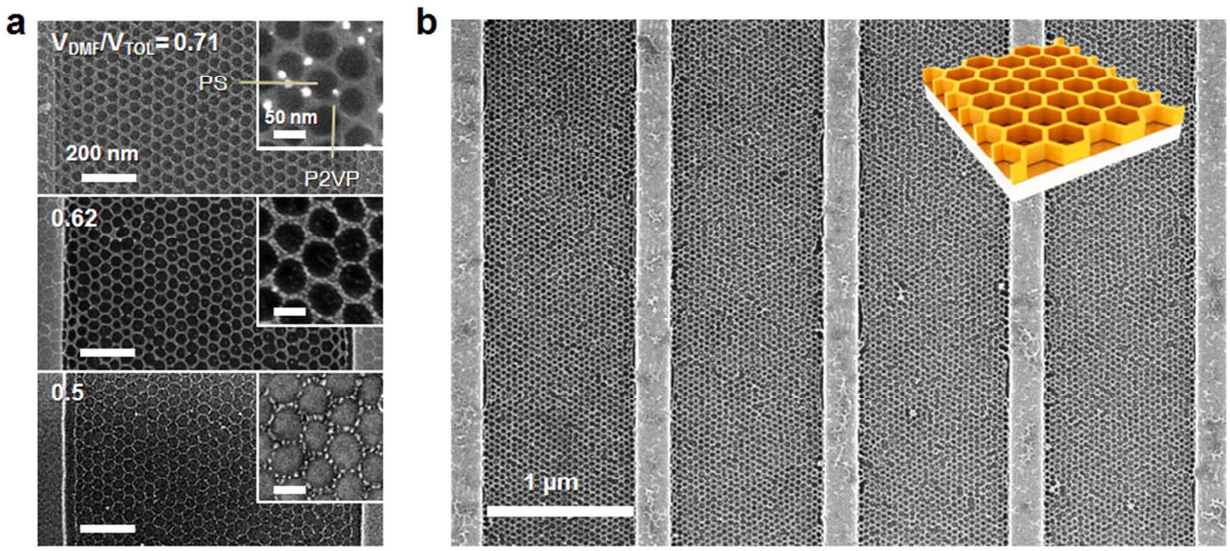

Fig. 2 Morphology control of the self-assembled hole structures (a) Precisely controlled hole structures from hole (top) to honeycomb (middle & bottom) depending on V_{DMF}/V_{TOL}, (b) SEM image of self-assembled honeycomb structure formed over the large area.

Nanoscale Accepted Manuscript

Nanoscale RSCPublishing

ARTICLE

We also investigated how mixed solvents of P2VP-preferential solvent (pyridine) and PS-preferential solvent (toluene) affect the self-assembly kinetics of PS-*b*-P2VP BCPs. In general, it is known that high-χ BCP shows slower self-assembly kinetics due to considerable decrease in the chain diffusivity with increase in χ. However, rapid and uniform pattern generation can be achieved *via* mixed solvent vapors treatments, which can provide better chain mobility than one solvent vapor annealing. While it took 90 minutes to get well-ordered line structures when pure toluene vapor was used for annealing SV42 BCP (Fig. S3), well-aligned pattern with a line-width of 12 nm was successfully accomplished within 10 minutes over the large area by annealing in the mixed solvents of pyridine and toluene (V_{PYR}/V_{TOL} =1) as shown in Fig. 3a and Fig. S4. Defect density of the self-assembled line structures decreases depending on the annealing time as shown Fig. 3c. Figs. 3b and 3d show how the volume ratio of pyridine and toluene (V_{PYR}/V_{TOL}) influences the ordering of the line patterns at a fixed annealing time of 10 minutes. As V_{PYR}/V_{TOL} ratio increases, the defect density dramatically decreases, showing highly-ordered line structures at V_{PYR}/V_{TOL} = 1. The reason for this is likely that the chain mobility of P2VP block can be kinetically disturbed by pure toluene vapor, because toluene is more preferential for PS block and therefore, chain mobility of P2VP block can be improved by adding P2VP-preferential solvent (pyridine or DMF) to toluene, which leads to a smaller activation barrier for chain diffusion.[4, 5]

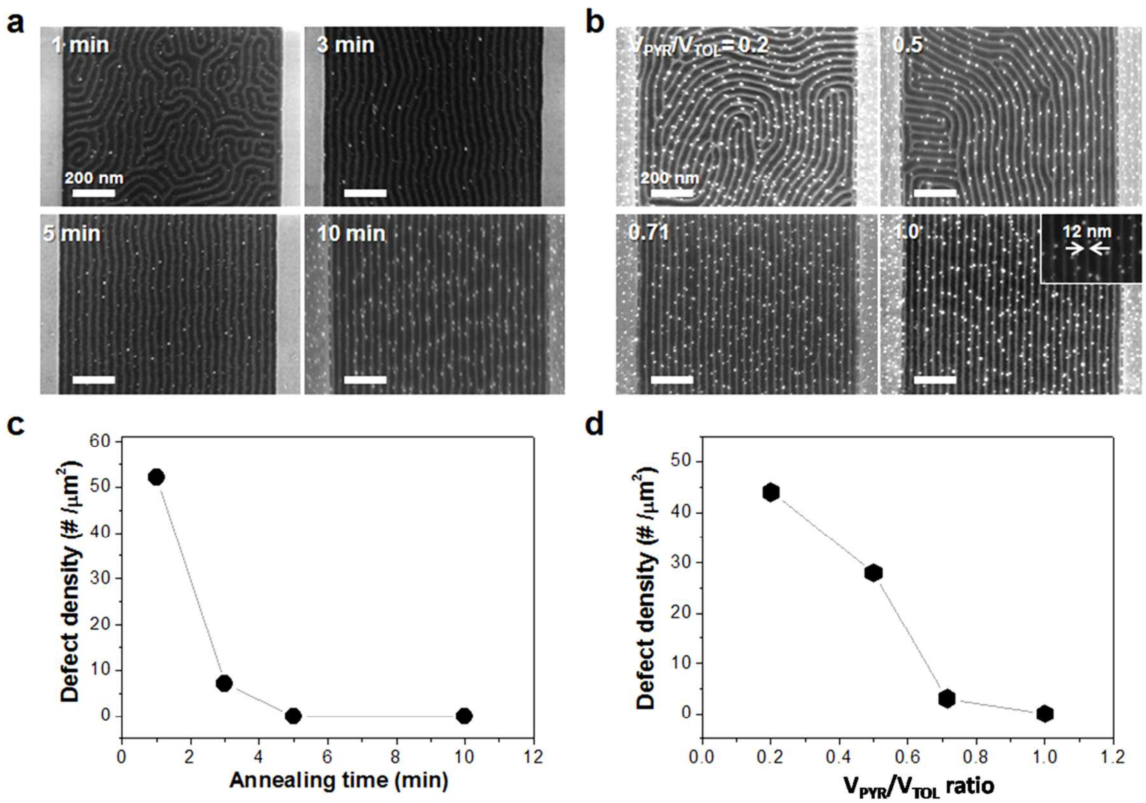

Fig. 3 Fast self-assembly kinetics for SV42 BCP. (a) Time evolution of self-assembled morphologies at V_{PYR}/V_{TOL} = 1, (b) Self-assembled morphologies at different V_{PYR}/V_{TOL} ratio and fixed annealing time of 10 min, (c) Defect density curve vs. annealing time at fixed at V_{PYR}/V_{TOL} = 1, (d) Defect density curve vs. V_{PYR}/V_{TOL} ratio.

Nanoscale Accepted Manuscript

This journal is © The Royal Society of Chemistry 2014

Nanoscale RSCPublishing

ARTICLE

The self-assembly time to obtain well-ordered structures can be further reduced for narrower guiding templates when annealed at mixed solvents of pyridine and toluene. Well-ordered 12-nm-line and ring structures in the line trench with a 300-nm-width (Fig. 4a, left) and circular hole-trench with 300-nm-diameter (Fig. 4a, right) were achieved within one minute of annealing time. This mixed solvents-induced rapid self-assembly of BCP is also applicable for other BCP with different MWs. For the PS-*b*-P2VP (SV34) with smaller MW of 34 kg/mol, we also explored the effect of mixed solvents (pyridine and toluene) on self-assembly kinetics. Fig. 4b (left) and Fig. S5 demonstrate that we can achieve highly-ordered 6-nm-line structures by adding pyridine solvent to toluene, showing fast self-assembly of SV34 BCP in a wide mixing range of V_{PYR}/V_{TOL} = 0.2 – 2.0 at a fixed annealing time of 5 min. This indicates that even a small portion of pyridine can significantly affect the self-assembly kinetics for smaller MW of BCP, lowering activation energy for chain diffusion.[36, 37] Furthermore, we also found that another solvent (DMF) which swells preferentially P2VP can speed up BCP self-assembly as shown in Fig. 4b (right). These results show that mixed solvents annealing using two solvents which consist of two preferentially swelling solvents for each block are greatly effective for achieving the fast self-assembly of BCPs *via* incorporation of preferential solvents into BCPs. In addition, it is also emphasized that this approach may be extensively utilized for diverse triblock BCPs (tri-BCPs) as well as diblock BCPs (di-BCPs) with high- χ such as poly(styrene-*b*-lactide) (PS-*b*-PLA), poly(styrene-*b*-ethylene oxide) (PS-*b*-PEO), poly(2vinylpyridine-*b*-dimethylsiloxane) (P2VP-*b*-PDMS), and poly(dimethylsiloxane-*b*-styrene) (PDMS-*b*-PS).

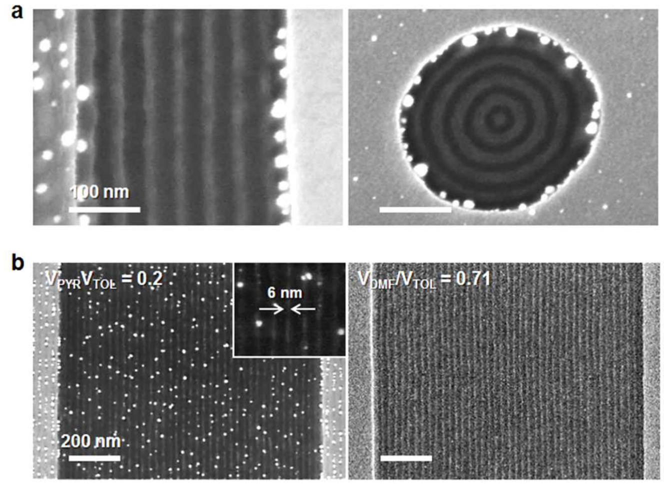

Fig. 4 Rapid pattern-formation of SV42 in the narrow trenches and sub-10 nm line structures of SV34. (a) Well-ordered 12-nm-line patterns from SV42 formed within 1 minute at V_{PYR}/V_{TOL} = 1 in the narrow trench. Trench width = 300 nm (left) & diameter = 250 nm (right), (b) 6-nm-line structures formed for 5 min at V_{PYR}/V_{TOL} = 0.2 (left) and V_{DMF}/V_{TOL} = 0.71 (right).

Methods

Self-assembly of block copolymers: Periodically lithography-patterned Si substrates with line and space trenches or circular holes were used as templates to guide the self-assembly of block copolymers (BCPs). The surface of the Si substrates was uniformly hydroxy-functionalized in order to promote self-assembly of BCPs. Hydroxy-terminated PS homopolymer with a molecular weight of 41 kg/mol dissolved in toluene was spin-coated on the Si substrates and annealed at 150 °C for 2 – 3 hours, and then washed with toluene. PS-*b*-P2VP BCPs dissolved in toluene were spin-coated on the PS-brush-treated Si substrates and annealed by appropriate solvent vapors. In order to explore the morphological transition and self-assembly kinetics of a PS-*b*-P2VP BCP (MW = 42 kg/mol), we used BCP solutions with two different weight percentages (1.0 wt% & 1.2 wt%) when spin-coating the solutions. More specifically, we used the BCP solution with 1.0 wt% to induce the morphological transition (cylinder-hole-lamella), whereas we used the BCP solution with 1.2 wt% to explain the self-assembly kinetics. The reason we

Nanoscale Accepted Manuscript

chose the BCP with 1.2 wt% for self-assembly kinetics study was because line structure is formed in the space region, while mesh or hole structure is created on the mesa region (Fig. S7). A stainless steel chamber (10 mL) with filled with a solvent or solvent mixture (6 mL) at the bottom was used for the annealing of BCPs. All the annealing process was conducted on the hot plate with a fixed temperature of 65°C to accelerate the kinetics of self-assembly. The annealed samples were immersed in the desired aqueous metal salt solution with hydrogen chloride (aq.) in the glass petri dish for 1 hour and washed by deionized water and then dried by blow with nitrogen gas. The BCP films were then etched by O_2 plasma at 30 sccm (gas flow rate), 10 m Torr (working pressure), 30 W (source power) for 30 sec to get the desired nanostructures using reactive ion etching (RIE) system in the Center for Nanoscale Materials (CNM) at Argonne National Laboratory. The small particles formed after O_2 plasma treatment were derived from metal incorporation (long immersion time of 1.5 hours). When the immersion time was optimized (30 minutes), the residual particles were not observed.

Conclusions

In summary, we have developed a tunable and rapid BCP self-assembly process using mixed solvent vapor annealing. Various nanostructures such as line, honeycomb, hole, and lamellar patterns were obtained from one cylinder-forming PS-*b*-P2VP BCP by precisely controlling the volume ratio of DMF and toluene. Pattern formation of 12-nm-width line was also effectively achieved within one minute *via* a mixed solvents treatment. This approach is expected to be extendable to other BCPs with different molecular weights and volume fraction, and various mixture-solvent annealing systems.

Acknowledgements

The work was supported by the U.S. Department of Energy, Office of Science, Materials Sciences and Engineering Division. Use of the Electron Microscopy Center (EMC) and Center for Nanoscale Materials (CNM) of Argonne National Laboratory for SEM and RIE experiments is gratefully acknowledged.

Notes and references

[a] *Materials Science Division, Argonne National Laboratory, Lemont, IL 60439, USA*

[b] *Nanoscience and Technology Division, Argonne National Laboratory (ANL), Lemont, IL 60439, USA*

**Corresponding author E-mail: hong@anl.gov*

† Electronic Supplementary Information (ESI) available: PDF material involves morphological transition of SV42 BCP (Fig. S1), metal-oxide line and hole structures (Fig. S2), time-evolution of self-assembled SV42 BCP using pure toluene (Fig. S3), rapidly formed 12-nm line pattern over large area (Fig. S4), 6-nm line pattern formation of SV34 BCP depending on the V_{PYR}/V_{TOL} (Fig. S5), rapidly formed 6-nm line pattern over large area (Fig. S6), and the comparison of the self-assembled nanostructures of lines within the trench and holes on mesa region (Fig. S7). See DOI: 10.1039/b000000x/

1 C. M. Garner, D. Herr, C. Krautschik, www.itrs.net/Links/2007ITRS/LinkedFiles/ERM/DSAR11%20082107.DOC, 2007.
2 P. Mansky, Y. Liu, E. Huang, T. P. Russell, C. J. Hawker. *Science,* 1997**,** ***275***, 1458.
3 S. O. Kim, H. H. Solak, M. P. Stoykovich, N. J. Ferrier, J. J. De Pablo, P. F. Nealey. *Nature,* 2003**,** ***424***, 411.
4 T. Thurn-Albrecht, J. Schotter, C. A. Kastle, N. Emley, T. Shibauchi, L. Krusin-Elbaum, K. Guarini, C. T. Black, M. T. Tuominen, T. P. Russell. *Science,* 2000**,** ***290***, 2126.
5 J. Y. Cheng, A. M. Mayes, C. A. Ross. *Nat. Mater.,* 2004**,** ***3***, 823.
6 M. P. Stoykovich, P. F. Nealey. *Mater. Today,* 2006**,** ***9***, 20.
7 I. Bita, J. K. W. Yang, Y. S. Jung, C. A. Ross, E. L. Thomas, K. K. Berggren. *Science,* 2008**,** ***321***, 939.
8 K. G. A. Tavakkoli, K. W. Gotrik, A. F. Hannon, A. Alexander-Katz, C. A. Ross, K. K. Berggren. *Science,* 2012**,** ***336***, 1294.
9 R. A. Segalman, H. Yokoyama, E. J. Kramer. *Adv. Mater.,* 2001**,** ***13***, 1152.
10 Q. Peng, Y. C. Tseng, S. B. Darling, J. W. Elam. *ACS Nano,* 2011**,** ***5***, 4600.
11 R. Ruiz, H. M. Kang, F. A. Detcheverry, E. Dobisz, D. S. Kercher, T. R. Albrecht, J. J. de Pablo, P. F. Nealey. *Science,* 2008**,** ***321***, 936.
12 J. Y. Cheng, D. P. Sanders, H. D. Truong, S. Harrer, A. Friz, S. Holmes, M. Colburn, W. D. Hinsberg. *ACS Nano,* 2010**,** ***4***, 4815.
13 J. W. Jeong, W. I. Park, M. J. Kim, C. A. Ross, Y. S. Jung. *Nano Lett.,* 2011**,** ***11***, 4095.
14 Y. S. Jung, C. A. Ross. *Nano Lett.,* 2007**,** ***7***, 2046.
15 C. M. Bates, T. Seshimo, M. J. Maher, W. J. Durand, J. D. Cushen, L. M. Dean, G. Blachut, C. J. Ellison, C. G. Willson. *Science,* 2012**,** ***338***, 775.
16 M. Muller, D. W. Sun. *Phys. Rev. Lett.,* 2013**,** ***111***, 267801.
17 J. K. Yang, Y. S. Jung, J. B. Chang, R. A. Mickiewicz, A. Alexander-Katz, C. A. Ross, K. K. Berggren. *Nat. nanotechnol.,* 2010**,** ***5***, 256.
18 M. P. Stoykovich, H. Kang, K. C. Daoulas, G. Liu, C. C. Liu, J. J. de Pablo, M. Mueller, P. F. Nealey. *ACS Nano,* 2007**,** ***1***, 168.
19 M. Y. Paik, J. K. Bosworth, D. M. Smilges, E. L. Schwartz, X. Andre, C. K. Ober. *Macromolecules,* 2010**,** ***43***, 4253.
20 T. Hirai, M. Leolukman, S. Jin, R. Goseki, Y. Ishida, M. A. Kakimoto, T. Hayakawa, M. Ree, P. Gopalan. *Macromolecules,* 2009**,** ***42***, 8835.
21 H. Y. Chris Benchera, Jessica Zhoua, Manping Caia, Jeffrey Smitha, Liyan Miaoa,, S. B. Ofir Montalb, Alon Laviab, Kfir Dotana, Huixiong Daia, D. P. S. a. M. T. Joy Y. Chengc, Steven Holmesd. *SIPE,* 2012**,** ***8323***.
22 W. I. Park, K. Kim, H. I. Jang, J. W. Jeong, J. M. Kim, J. Choi, J. H. Park, Y. S. Jung. *Small,* 2012**,** ***8***, 3762.
23 X. Zhang, K. D. Harris, N. L. Wu, J. N. Murphy, J. M. Buriak. *ACS Nano,* 2010**,** ***4***, 7021.
24 C. A. Ross, K. K. Berggren, J. Y. Cheng, Y. S. Jung, J. B. Chang. *Adv. Mater.,* 2014.
25 C. T. Black, R. Ruiz, G. Breyta, J. Y. Cheng, M. E. Colburn, K. W. Guarini, H. C. Kim, Y. Zhang. *IBM J. Res. Dev.,* 2007**,** ***51***, 605.
26 D. J. C. Herr. *J. Mater. Res.,* 2011**,** ***26***, 122.
27 D. Borah, M. T. Shaw, J. D. Holmes, M. A. Morris. *ACS Appl. Mater. Interfaces,* 2013**,** ***5***, 2004.
28 K. W. Gotrik, C. A. Ross. *Nano Lett.,* 2013**,** ***13***, 5117.

Nanoscale Accepted Manuscript

 This journal is © The Royal Society of Chemistry 2014

29 J. H. Mun, Y. H. Chang, D. O. Shin, J. M. Yoon, D. S. Choi, K. M. Lee, J. Y. Kim, S. K. Cha, J. Y. Lee, J. R. Jeong, Y. H. Kim, S. O. Kim. *Nano Lett.*, 2013, ***13***, 5720.
30 D. O. Shin, J. H. Mun, G. T. Hwang, J. M. Yoon, J. Y. Kim, J. M. Yun, Y. B. Yang, Y. Oh, J. Y. Lee, J. Shin, K. J. Lee, S. Park, J. U. Kim, S. O. Kim. *ACS Nano*, 2013, *7*, 8899.
31 S. J. Jeong, J. Y. Kim, B. H. Kim, H. S. Moon, S. O. Kim. *Mater. Today*, 2013, ***16***, 468.
32 J. Bang, S. H. Kim, E. Drockenmuller, M. J. Misner, T. P. Russell, C. J. Hawker. *J. Am. Chem. Soc.,* 2006**,** ***128***, 7622.
33 S. Park, D. H. Lee, J. Xu, B. Kim, S. W. Hong, U. Jeong, T. Xu, T. P. Russell. *Science,* 2009**,** ***323***, 1030.
34 Y. S. Jung, C. A. Ross. *Adv. Mater.,* 2009**,** ***21***, 2540.
35 Y. Wu, G. Cheng, K. Katsov, S. W. Sides, J. Wang, J. Tang, G. H. Fredrickson, M. Moskovits, G. D. Stucky. *Nat. Mater.,* 2004**,** ***3***, 816.
36 G. Kim, M. Libera. *Macromolecules,* 1998**,** ***31***, 2670.
37 J. N. L. Albert, T. D. Bogart, R. L. Lewis, K. L. Beers, M. J. Fasolka, J. B. Hutchison, B. D. Vogt, T. H. Epps. *Nano Lett.,* 2011**,** ***11***, 1351.
38 W. I. Park, Y. Kim, J. W. Jeong, K. Kim, J. K. Yoo, Y. H. Hur, J. M. Kim, E. L. Thomas, A. Alexander-Katz, Y. S. Jung. *Scientific reports,* 2013**,** ***3***, 3190.
39 T. P. Lodge, M. C. Dalvi. *Phys. Rev. Lett.,* 1995**,** ***75***, 657.
40 R. Ruiz, J. K. Bosworth, C. T. Black. *Phys. Rev. B,* 2008**,** ***77***, 054204.
41 M. R. Hammond, E. Cochran, G. H. Fredrickson, E. J. Kramer. *Macromolecules,* 2005**,** ***38***, 6575. 38 M. R. Hammond, E. Cochran, G. H. Fredrickson, E. J. Kramer. *Macromolecules,* 2005**,** ***38***, 6575.
42 M. W. Matsen, F. S. Bates. *Macromolecules*, 1996, ***29***, 7641.
43 J. Chai, D. Wang, X. Fan, J. M. Buriak. *Nat. nanotechnol.,* 2007**,** ***2***, 500.

Nanoscale Accepted Manuscript